Astron. Astrophys. 333, 27–30 (1998)

ASTRONOMY AND ASTROPHYSICS

Three-dimensional dynamos in spiral galaxies

R. Rohde and D. Elstner

Astrophysikalisches Institut Potsdam, An der Sternwarte 16, D-14482 Potsdam, Germany

Received 28 October 1997 / Accepted 28 January 1998

Abstract. Solutions of the 3D nonlinear induction equation for dynamos in spiral galaxies are presented in this paper. Our model includes differential rotation, ambipolar diffusion and, based on small-scale turbulence, eddy diffusivity and the tensorial α–effect underlying magnetic feedback. The nonaxisymmetric radial-azimuthal spiral pattern and the vertical stratification of the galaxy are represented in the density and turbulence profile.

Our calculations are chiefly concerned with the effect of field concentration between (or within) the spiral arms. The possible induction of bisymmetric instead of axisymmetric structured fields is also investigated.

We distinguish between models with weak and strong turbulence contribution, that is small and large correlation time $\tau_{\rm corr}$ of interstellar turbulence. For small correlation times we find axisymmetric steady solutions of even parity showing concentration between the spiral arms. The pitch angles are relatively large and increase with enlarged correlation time. Large correlation times are linked with oscillating BSS type solutions of again even parity, but they are clearly concentrated within the spiral arms.

Key words: *magnetohydrodynamics* (MHD) – turbulence – ISM: magnetic fields – galaxies: ISM

1. Introduction

It is known from radio polarization observations that spiral galaxies own large-scale magnetic fields of different, but in the most cases spiral geometry (Beck et al. 1996). Two basic field properties are of interest respecting the spiral field geometry: i) The field concentration between spiral arms as it is observed in the case of NGC 6946 (Beck & Hoernes 1996); ii) The appearance of axisymmetric (ASS) and bisymmetric spiral structured fields (BSS). The latter seems to be rather seldom and is observed in e.g. M 81 (Beck et al. 1996). The mechanisms concerning such properties of galactic magnetic fields are still not satisfactorily investigated. The basic ansatz for those investigations is a nonaxisymmetry in the underlying galaxy model, whereas the discussed mechanisms are of different origin (Beck et al. 1996; Moss 1997a). Therefore a 3D analysis is unavoidable.

So far applied 2D (Moss 1996, 1995) and 3D simulations (Moss 1997b; Otmaniowska-Mazur & Chiba 1995; Moss et al. 1993; Panesar & Nelson 1992) were mostly concerned with mechanisms leading to a nonaxisymmetric gas velocity, whereby restrictions were used as neglecting vertical stratifications, discussing linear theory or evaluating solutions restricted to symmetry conditions. Further turbulence effects as diamagnetism and buoyancy were then neglected. This situation is also found in simulations which investigate nonaxisymmetric turbulence coefficients (Moss 1996; Moss et al. 1993).

Since most investigations (Moss et al. 1993; Moss 1995, 1996) chiefly discussed the induction of BSS type fields we lay in this paper emphasis on the effect of field concentration between spiral arms, respecting the observations made for NGC 6946; but we also touch the discussion about inducing ASS versus BSS type fields.

In our models the built-in nonaxisymmetry is attached to the density profile and the turbulence contribution. The density stratification is taken from observational results and is used as a base for the calculated vertical turbulence profile in order to represent the galactic properties most realistic in a consistent manner. The α-tensor includes a consistent feedback mechanism of the magnetic field (Rüdiger & Kitchatinov 1993); but we neglect the feedback onto the eddy diffusivity. We do not follow the concept of solving both the induction and the Navier-Stokes equation (Barker & Moss 1994) as we neglect influence of the magnetic field onto the gas velocity. Our 3D time-stepping code (Elstner et al. 1990; Rohde et al. 1998) uses cylindrical polar coordinates and allows a nonlinear treatment without restrictions onto the symmetry of the solutions.

2. The mean-field electrodynamics

The evolution of the mean magnetic field $\bar{\boldsymbol{B}}$ is governed by the dynamo equation

$$\frac{\partial \bar{\boldsymbol{B}}}{\partial t} = \mathrm{rot}\,(\bar{\boldsymbol{u}} \times \bar{\boldsymbol{B}} + \boldsymbol{u}_{\rm drift} \times \bar{\boldsymbol{B}} + \boldsymbol{\mathcal{E}}), \qquad (1)$$

where $\boldsymbol{\mathcal{E}}$ is the turbulent electromotive force, $\boldsymbol{\mathcal{E}} = \langle \boldsymbol{u}' \times \boldsymbol{B}' \rangle$, and $\bar{\boldsymbol{u}} = (0, r\Omega(r), 0)$ the mean velocity of the differentially rotating interstellar gas (Krause & Rädler 1980).

Send offprint requests to: D. Elstner

2.1. The turbulent EMF

As usual, we assume approximate scale separation and write

$$\mathcal{E}_i = \alpha_{ij}\bar{B}_k + \eta_{ijk}\bar{B}_{j,k}. \tag{2}$$

The α-tensor takes the form

$$\alpha_{ij} = \begin{pmatrix} \alpha_{rr} & -(U_z^{\rm dia}+U_z^{\rm buo}) & (U_\phi^{\rm dia}+U_\phi^{\rm buo}) \\ (U_z^{\rm dia}+U_z^{\rm buo}) & \alpha_{\phi\phi} & -(U_r^{\rm dia}+U_r^{\rm buo}) \\ -(U_\phi^{\rm dia}+U_\phi^{\rm buo}) & (U_r^{\rm dia}+U_r^{\rm buo}) & \alpha_{zz} \end{pmatrix} \tag{3}$$

with diagonal terms

$$\alpha_{rr} = \alpha_{\phi\phi} = -\frac{4}{5}\tau_{\rm corr}^2\Omega\tilde{\Psi}\left(\langle \boldsymbol{u}'^2\rangle\frac{\partial}{\partial z}\log\rho + \frac{1}{3}\frac{\partial}{\partial z}\langle \boldsymbol{u}'^2\rangle\right), \tag{4}$$

$$\alpha_{zz} = \frac{4}{5}\tau_{\rm corr}^2\Omega\tilde{\Psi}_z\left(\frac{1}{3}\langle \boldsymbol{u}'^2\rangle\frac{\partial}{\partial z}\log\rho + \frac{2}{3}\frac{\partial}{\partial z}\langle \boldsymbol{u}'^2\rangle\right), \tag{5}$$

turbulent diamagnetism

$$\boldsymbol{U}^{\rm dia} = -\frac{c_\eta}{2}\Psi_{\rm dia}\tau_{\rm corr}\nabla\langle \boldsymbol{u}'^2\rangle \tag{6}$$

and magnetic buoyancy

$$\boldsymbol{U}^{\rm buo} = \langle \boldsymbol{u}'^2\rangle\Psi_{\rm buo}\tau_{\rm corr}\nabla\log\rho. \tag{7}$$

Notice that the EMF varies with r, φ and z. This is caused by the nonaxisymmetry and the stratification in density and turbulent velocity (cf. Sect. 3.2 and 3.3 below). We simulate the nonaxisymmetric galactic pattern with enhanced density and turbulent velocity within the spiral arms. The different quenching functions Ψ represent the influence of the magnetic field strength β onto the turbulence effects. The field strength β is defined as $\beta = |\bar{\boldsymbol{B}}|/B_{\rm eq}$ with the equipartition field

$$B_{\rm eq} = \sqrt{4\pi\rho\langle \boldsymbol{u}'^2\rangle}. \tag{8}$$

A more detailed description of the EMF and the corresponding quenching functions are given in Elstner et al. (1996) and Kitchatinov & Rüdiger (1993).

In our calculations we have neglected any feedback of the magnetic field itself onto the eddy diffusivity. The scalar field $\eta_{\rm T}$ is then given as

$$\eta_{\rm T} = c_\eta\langle \boldsymbol{u}'^2\rangle\tau_{\rm corr}. \tag{9}$$

2.2. Ambipolar diffusion

The ambipolar drift velocity is proportional to the Lorentz force,

$$\boldsymbol{u}_{\rm drift} = \frac{1}{4\pi\rho_i\nu_{\rm in}}\ {\rm rot}\,\bar{\boldsymbol{B}}\times\bar{\boldsymbol{B}}. \tag{10}$$

The mass density of ions is ρ_i and $\nu_{\rm in}$ is the ion-neutral collision frequency. In the following we set

$$\rho_i \simeq 10^{-26}\ {\rm g/cm^3}, \qquad \nu_{\rm in} \simeq 1.3\cdot 10^{-7}\ {\rm s^{-1}} \tag{11}$$

(Brandenburg & Zweibel 1995).

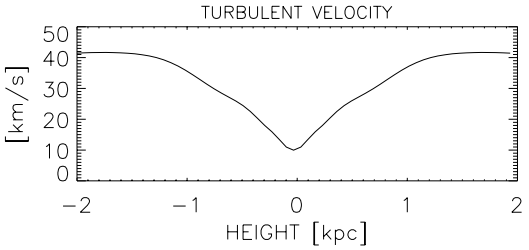

Fig. 1. The maximal turbulent velocity calculated from Eq. (16).

3. The model

3.1. Differential rotation

We consider galaxies to be differentially rotating turbulent disks embedded in a plasma of given conductivity (Elstner et al. 1990). In the simplest case the "plasma" is vacuum and the conductivity therefore vanishes. The thickness of the galaxy, H, is 4 kpc, its radius, $r_{\rm max}$, is 7.5 kpc.

The differentially rotating gas is described by a Brandt-type law with n = 2 (Donner & Brandenburg 1990; Sofue 1996) and r_Ω = 2 kpc,

$$\Omega = \Omega_0\left(1+\left(\frac{r}{r_\Omega}\right)^n\right)^{-1/n}. \tag{12}$$

Thus the velocity in the outer part of the galaxy doesn't exceed

$$V = r_\Omega\Omega_0. \tag{13}$$

We assume this velocity to have the same value (V = 100 km s^{-1}) in all our models.

3.2. Nonaxisymmetry

In order to take into account the influence of the spiral arms in density and diffusivity the profiles used by Otmianowska-Mazur & Chiba (1995) are adopted,

$$\mathcal{Q}_{\rm i} = 1 + \frac{q_{\rm i}-1}{2}\Big[1 + \cos\Big(2(\phi-\Omega_{\rm p}t) + 2\log\frac{r}{r_0}\cot\chi\Big)\Big], \tag{14}$$

varying between 1 and $q_{\rm i}$. The profile $\mathcal{Q}_{\rm i}$ is used for the density ($\mathcal{Q}_\rho$ with q_ρ) as well as for the turbulence intensity ($\mathcal{Q}_{\rm u}$ with $q_{\rm u}$)

$$\rho = \rho_0(z)\ \mathcal{Q}_\rho(r,\phi,t),$$
$$\langle \boldsymbol{u}'^2\rangle = \langle \boldsymbol{u}_0(z)'^2\rangle\ \mathcal{Q}_{\rm u}(r,\phi,t). \tag{15}$$

$\Omega_{\rm p}$ is the angular pattern speed of the $m = 2$ spiral and is set to 13 Gyr^{-1} in all calculations. The density contrasts $\mathcal{Q}_{\rm i}$ are fixed with $q_{\rm i} = 5$. The pitch angle χ is taken as 25° in the present paper.

3.3. Vertical stratification

For the density stratification we take the empirical H I distribution of Dickey & Lockmann (1990) as an ansatz for our simplified galaxy model: a combination of two Gaussians of central

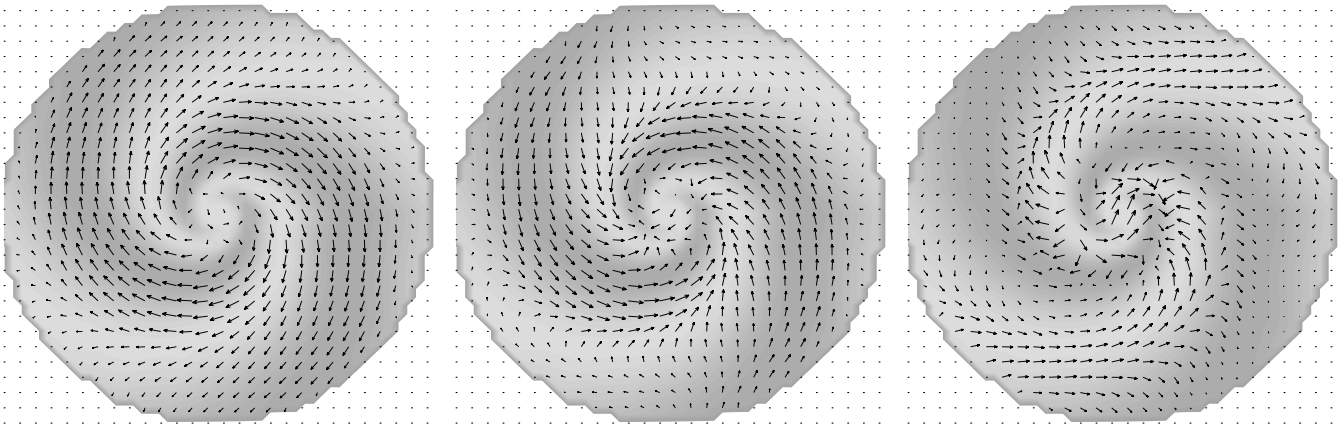

Fig. 2. Magnetic field geometry for LEFT: $\tau_{\rm corr}$ = 30 Myr (after 3.3 Gyr), MIDDLE: $\tau_{\rm corr}$ = 50 Myr (after 3.3 Gyr), RIGHT: $\tau_{\rm corr}$ = 100 Myr (after 2.0 Gyr). The optical spiral arms are shown in light grey.

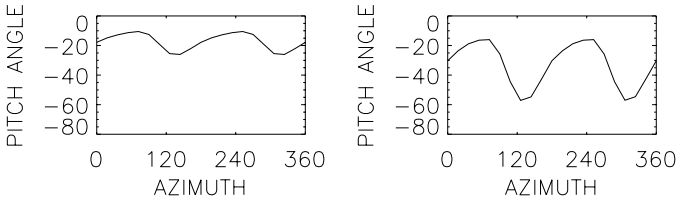

Fig. 3. Magnetic pitch angles in the mid-plane at $r = r_{\rm max}/2$ for LEFT: $\tau_{\rm corr}$ = 30 Myr, RIGHT: $\tau_{\rm corr}$ = 50 Myr. (Both after 3.3 Gyr.)

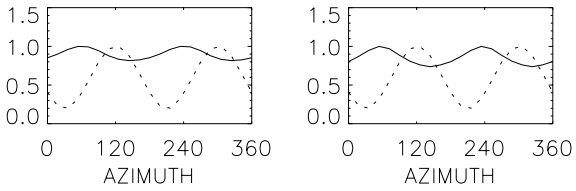

Fig. 4. Normalized field strength (solid) compared with density profile (dotted) for LEFT: $\tau_{\rm corr}$ = 30 Myr, RIGHT: $\tau_{\rm corr}$ = 50 Myr. (Position and time as in Fig. 3.)

densities 0.395 and 0.107 cm^{-3} and scale heights of 212 and 530 pc respectively, and an exponential with central density 0.064 cm^{-3} and a scale height of 403 pc. Then we have added a further Gaussian with mid-plane density 0.3 H_2 cm^{-3} and dispersion 70 pc to include the molecular gas layer (cf. Bloemen 1987), and an exponential with scale height 1.5 kpc and a mid-plane density of 0.025 cm^{-3} representing the extended ionized gas (Reynolds 1989). For sake of simplicity we assume that profile being valid in all parts of the galaxy.

Based on the given density stratification we take a common simplification of the vertical momentum equation as a possibility to calculate the turbulence intensity:

$$\frac{d}{dz}\left(\rho_0(z)\langle \boldsymbol{u}_0(z)'^2\rangle\right) = -\rho_0(z)k_z \tag{16}$$

The used potential k_z is essentially due to a self-gravitating isothermal sheet of stars with constant thickness z_0

$$k_z(z) = \frac{2\sigma^2}{z_0}\tanh\left(\frac{z}{z_0}\right). \tag{17}$$

Again for sake of simplicity all radial dependencies are neglected. We set σ = 21.5 km s^{-1} being the vertical velocity dispersion of the old disk stars and z_0 = 0.6 kpc. For details see Fröhlich & Schultz (1996) and Elstner et al. (1996). The mid-plane turbulent velocity was assumed to be 10 km s^{-1}.

The resulting vertical profile of the turbulent velocity we used in all our models is shown in Fig. 1.

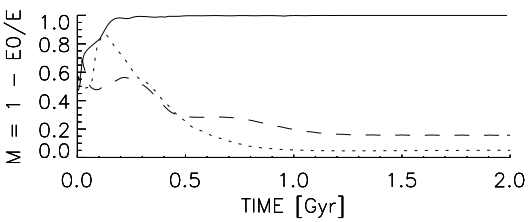

Fig. 5. Symmetry parameter M for $\tau_{\rm corr}$ = 100 Myr (solid) compared with the ASS type solutions for $\tau_{\rm corr}$ = 50 Myr (dashed) and $\tau_{\rm corr}$ = 30 Myr (dotted).

4. Results

We compare dynamo models for different correlation times of interstellar turbulence $\tau_{\rm corr}$, which we take as a free parameter without discussing the physical origin of the turbulence.

In all our simulations we used a small seed field being a combination of a $m = 0$ and $m = 1$ mode and also being a mixture of a symmetric and an antisymmetric field component with respect to the galactic mid-plane. Using the symmetry parameter $M = 1 - E_0/E$ and the parity parameter $P = (E_{\rm S} - E_{\rm A})/(E_{\rm S} + E_{\rm A})$ with E total energy of the field, E_0 energy of its axisymmetric part, $E_{\rm A}$ and $E_{\rm S}$ energy of the even and odd field components respectively, the seed field has the values $P = 0$ and $M = 0.5$ at time $t = 0$.

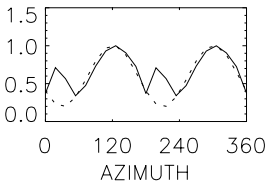

Fig. 6. Normalized field strength (solid) compared with density profile (dotted) in the mid-plane at $r = r_{\max}/2$ for $\tau_{\rm corr}$ = 100 Myr (after 2 Gyr).

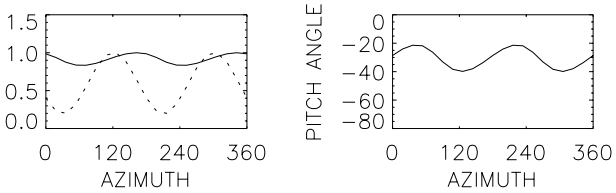

Fig. 7. A model with axisymmetric turbulence contribution ($\mathcal{Q}_{\rm u}$ = const., cf. Eq. 15): LEFT: Normalized field strength (solid) compared with density profile (dotted), RIGHT: Magnetic pitch angles . $\tau_{\rm corr}$ = 50 Myr. Located in the mid-plane at $r = r_{\max}/2$, after 3.42 Gyr.

4.1. ASS type fields between spiral arms

Models based on relative small correlation times lead to steady S0 solutions (Fig. 2, Fig. 5). The dynamo growth times are about 1.5 to 2 Gyr.

In case of $\tau_{\rm corr}$ = 30 Myr, which is the common standard value, we achieve magnetic pitch-angles varying between 10° in the interarm region to 30° in the spirals (Fig. 3). The field strength shows concentration in the interarm region (Fig. 4).

For larger correlation times (50 Myr) we receive solutions with a more complicated geometry: The magnetic field in the very inner part of the galaxy has bisymmetric structure and rotates with a period of about 4 Gyr. In the outer parts a steady field is excited that is dominated by a S0 mode. The magnetic pitch angles vary between 60° in the spirals and 20° between the spirals (Fig. 3). The field concentration between the spiral arms is weakly enlarged in comparison to the model with smaller correlation time (Fig. 4). The magnetic field strength variation reaches a value of almost 30%. Having in mind that the intensity of synchrotron radiation goes roughly with B^4 (equilibrium with cosmic rays assumed), already 20% variation in B would explain the magnetic arms in e.g. NGC 6946 (cf. Beck & Hoernes 1996).

In the models with relative small correlation times the field generation seems rather based on the differential rotation that affects the dynamo induced field all over the galactic plane, whereas the diffusivity weakens the field more intensively in the spiral arms.

4.2. BSS type fields within spiral arms

In case of a large correlation time (100 Myr) the type of the dynamo changes significantly. This model leads to a S1 dynamo solution (Fig. 2, Fig. 5). Its magnetic field is clearly concentrated within the spiral arms (Fig. 6). The solution is oscillating and therefore the magnetic pitch angle varies in time.

The dynamo growth time for this model is very short being about 0.1 Gyr.

We interpret this behaviour as being due to the strong α-effect that works mostly in the spiral arms where the turbulent velocity is assumed as large.

Taking into account the estimation that α should not exceed the turbulent velocity u' (cf. Beck et al. 1996), we should note that such a model is in this sense very artificial.

4.3. The role of nonaxisymmetric contributions

It can be seen from the dynamo equation that the influence of the spiral galactic profile onto the induced magnetic field is essentially based on the spiral contribution of the turbulence. The density profile contributes only via magnetic feedback, which is based on the field strength β including the equipartition field $B_{\rm eq}$, and via magnetic buoyancy. Considering an artificial model with $\tau_{\rm corr}$ = 50 Myr having an axisymmetric turbulence ($\mathcal{Q}_{\rm u}$ = const., cf. Eq. 15) but nonaxisymmetric density profile we indeed achieve a steady S0 solution with a weak field concentration and dilution respectively where the density varies most strongly (Fig. 7).

Neglecting the radial-azimuthal density profile ($\mathcal{Q}_\rho$ = const., cf. Eq. 15) however does not show a significant effect since the field generation seems to be dominated by the turbulence contribution.

Acknowledgements. We thank the Deutsche Forschungsgemeinschaft for support (project Ru 488/7).

References

Barker D.M., Moss D., 1994, A&A 283, 1009
Beck R. & Hoernes P., 1996, Nat 379, 47
Beck R., Brandenburg A., Moss D., Shukurov A., Sokoloff D.D., 1996, Annual Rev. A&A 34, 155
Bloemen J.B.G.M., 1987, ApJ 322, 694
Brandenburg A., Zweibel E.G., 1995, ApJ 448, 734
Dickey J.M., Lockmann F.J., 1990, ARA&A 28, 215
Donner K.J., Brandenburg A., 1990, A&A 240, 289
Elstner D., Meinel R., Rüdiger G., 1990, GAFD 50, 85
Elstner D., Rüdiger G., Schultz M., 1996, A&A 306, 740
Fröhlich H.-E., Schultz M., 1996, A&A 311, 451
Krause F., Rädler K.-H., 1980, Mean-field magnetohydrodynamics and dynamo theory. Akademie-Verlag, Berlin
Moss D., 1995, MNRAS 275, 191
Moss D., 1996, A&A 315, 63
Moss D., 1997a, Contemporary Physics, vol. 38, no. 1, p. 49
Moss D., 1997b, MNRAS 289, 554
Moss D., Brandenburg A., Donner K.J., Thomasson M., 1993, ApJ 409, 179
Otmianowska-Mazur K., Chiba M., 1995, A&A 301, 41
Panesar J.S. & Nelson A.H., 1992, A&A 264, 77
Reynolds R.J., 1989, ApJ 339, L29
Rohde R., Elstner D., Rüdiger G., 1998, A&A 329, 911
Rüdiger G. & Kitchatinov L.L., 1993, A&A 269, 581
Sofue Y., 1996, ApJ 458, 120